Time-dependent quantum current for independent electrons driven under nonperiodic conditions

X. Oriols,* A. Alarcón, and E. Fernàndez-Díaz
Departament d'Enginyeria Electrònica, ETSE, Universitat Autònoma de Barcelona 08193, Bellaterra, Barcelona, Spain
(Received 25 October 2004; revised manuscript received 24 February 2005; published 24 June 2005)

An expression for the computation of the current in phase-coherent devices driven under arbitrarily time-dependent conditions is presented. The approach is developed for independent electrons in the time domain within a first-quantization formalism. The time-dependent current is computed by generalizing the Ramo-Shockley theorem to quantum systems. It is shown that the time-dependent conductance is not proportional to the quantum transmission coefficient, but to a parameter named the quantum current coefficient. As a test, it is proved that the present approach leads to the well-known Landauer model when static potentials are considered. As a simple numerical example, coherent quantum pumping is studied and applications for nanoscale solid-state field-effect transistors are predicted.

DOI: 10.1103/PhysRevB.71.245322 PACS number(s): 73.40.Gk, 72.30.+q, 05.60.Gg, 73.23.−b

I. INTRODUCTION

Investigation of quantum phenomenology in time-dependent scenarios reveals information not available from dc transport.[1–21] However, such investigation is a really hard task, from either an experimental[19–21] or a theoretical point of view.[1–18] The modeling of fast-varying time-dependent systems cannot rely on Hamiltonian eigenstates because the electron energy is no longer a constant of motion. When traversing the time-dependent system, the electron exchanges its energy with the oscillating system and it emerges at the opposite contact with a different value. In addition, the experimental current depends not only on the conduction current, but also on the displacement current which is originated by temporal variations of the electric fields.[16,17,22] Moreover, such temporal variations of the electric field can generate a time-dependent magnetic field that leads to the propagation of electromagnetic energy through the system.[22] Thus, trying to develop a general quantum transport theory for time-dependent Hamiltonians is, indeed, a hopeless task without some serious approximations.

In this work, we compute the quantum current in phase-coherent devices driven under arbitrarily time-dependent potentials. Our approach computes the quantum current density for a flux of independent particles and uses the Ramo-Shockley theorem[23–26] to calculate the current in quantum systems. The model has been developed having in mind nanoscale solid-state field-effect transistors.[27] As seen in Fig. 1, the electron transport occurs from the source to the drain reservoirs, both biased at a constant voltage. The source-drain conductance is controlled by a gate contact with a time-dependent bias. The approach presented here can be straightforwardly generalized to other devices such as laser-controlled molecular wires,[28] carbon nanotube transistors,[29] etc.

A review of several theoretical techniques used to study transport in time-dependent nanoscale systems can be found in recent work of Platero and Aguado.[1] Most of the models are developed in the energy domain (within a scattering matrix formalism[2–15,28,30]). In particular, an important effort was made by Buttiker and co-workers[11–15] to provide fully quantum theories for phase-coherent devices under ac conditions taking into account the Poisson equation. They succeeded in extending the Landauer approach to time-dependent mesoscopic systems assuring overall current and charge conservation under ac conditions in the adiabatic limit (where any kinetic electron time associated with the device is much shorter than the reciprocal of the external ac frequency). Let us emphasize that the previous approach can be applied to systems where all contacts are biased with time-dependent voltages. Here, on the contrary, we assume that the source-drain terminals are biased at constant voltages. The approach of Buttiker and co-workers has been successfully used by Brouwer[31] to study pumping currents, but it is only valid for slowly changing voltages where the system is driven adiabatically through a sequence of quasistatic scenarios (i.e., the adiabatic limit).

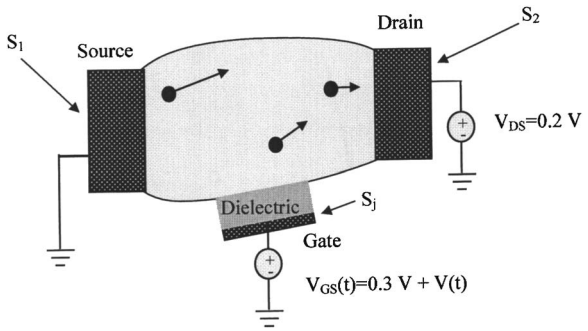

FIG. 1. Schematic transistor representation. The drain-source current is controlled by the Coulomb interaction between electrons in the system and those at the gate contact, which are separated by a dielectric region. A constant $V_{DS}=0.2$ V is applied from drain to source. The gate contact is biased at a time-dependent voltage $V_{GS}(t)=(0.3\ \mathrm{V})+V(t)$.

On the other side, the Floquet formalism[3–7] is the standard energy-domain method used to study the nonadiabatic limit (when the electron dwell time is comparable to or larger than the temporal variations of the potential). Quantum tunneling phenomenology is enriched in this limit.[8–10,32–37] The Floquet formalism is used for the periodic Hamiltonian $\hat{H}(t)=\hat{H}(t+T)$, where T is the period. The Floquet theorem[3–7]

states that the solutions of the Schrödinger equation in a time-periodic potential can be described as a linear combination of Floquet states (such Floquet states play a role similar to the Bloch states in spatially periodic Hamiltonians). Elaborated models using the Floquet formalism have been developed to deal with coherent quantum pumping,[3,7,32–34] coherent destruction of tunneling,[8,9] or current fluctuations.[30] However, the Floquet theory is only valid for time-periodic Hamiltonians. For example, the quantum transient current response to step voltage transitions (i.e., digital application of nanoscale quantum devices) cannot be studied with the previous Floquet formalism.

Here, we develop an alternative approach that can be applied for arbitrarily time-dependent potential profiles (in either adiabatic or nonadiabatic conditions) with a quite simple numerical implementation. Our approach computes the quantum current density for a flux of independent particles and uses the Ramo-Shockley theorem[23–26] to define the experimentally measured current in quantum systems. As we have mentioned, the approach is developed in the time domain. Such studies were initiated by Kulander in 1987 while investigating laser-atom interactions.[35] An instructive comparison of wave-packet and Floquet formalisms in laser-atom scenarios can be found in Ref. 7. A scattering matrix theory in the time domain has also been formulated by Vavilov *et al.*[18] In the authors' opinion, exploring the delicate time-dependent tunneling phenomenology within both (energy and time) domains can result in a complementary and fruitful understanding.

The rest of the paper is divided as follow. In Sec. II, we rewrite the Ramo-Shockley theorem in terms of the conduction current density and the electromagnetic potentials, and we discuss some simplifying assumptions. Then, in Sec. III, we present the computation of the quantum time-dependent current for time-dependent Hamiltonians (the main result of this work). After that, in Sec. IV, we show how our formalism exactly reproduces the Landauer model when static potentials are considered. In Sec. V, we present numerical results developed for field-effect solid-state transistors and we discuss possible applications. We conclude in Sec. VI. Finally, two appendixes discuss numerical details.

II. THE RAMO-SHOCKLEY THEOREM

In order to provide a comprehensive derivation of the time-dependent quantum current, we rewrite the Ramo-Shockley theorem[23–26] in terms of the conduction current and the electromagnetic potentials. We follow the development of Pellegrini.[25,26]

A. The Ramo-Shockley theorem in terms of conduction current and electromagnetic potentials

We define a particular volume Ω (for example, $\Omega = L_z L_y L_z$ in Fig. 2) that contains the whole device active region and a surface S that limits this volume. This surface S is divided into M smaller surfaces named S_h. A vector function $\vec{F}_i(\vec{r})$ inside the volume Ω is defined through the expression

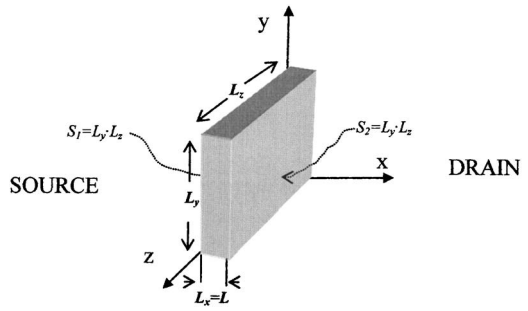

FIG. 2. Schematic representation of the 3D device geometry considered in this work. Electron transport from source (S_1) to drain (S_2) surfaces is considered. A time-dependent gate bias is considered at some of the other surfaces. These surfaces are considered much smaller than S_1 and S_2 within the assumption $L_x \ll L_y, L_z$.

$\vec{F}_i(\vec{r}) = -\vec{\nabla}\Phi_i(\vec{r})$ where the scalar function $\Phi_i(\vec{r})$ is the solution of the Laplace equation

$$\vec{\nabla}[\varepsilon(\vec{r})\vec{F}_i(\vec{r})] = -\vec{\nabla}[\varepsilon(\vec{r})\vec{\nabla}\Phi_i(\vec{r})] = 0 \tag{1}$$

for the particular boundary condition at the surface $\Phi_i(\vec{r}) = 1, \vec{r} \in S_i$, and zero elsewhere, i.e., $\Phi_i(\vec{r}) = 0, \vec{r} \in S_{h\neq i}$. For simplicity, the electric permittivity $\varepsilon(\vec{r})$ is assumed to be a time independent scalar function. The functions $\vec{F}_i(\vec{r})$ and $\Phi_i(\vec{r})$ can be interpreted as the electric field and the scalar potential, respectively, present in Ω without charge (when the previous particular boundary conditions are considered). Therefore, the total time-dependent current $I_i(t)$ through the particular surface S_i can be obtained from the following integral:

$$\begin{aligned}\int_\Omega \vec{F}_i(\vec{r})\cdot\vec{J}(\vec{r},t)d^3\vec{r} &= \int_\Omega \vec{F}_i(\vec{r})\cdot\vec{J}_c(\vec{r},t)d^3\vec{r} \\ &+ \int_\Omega \vec{F}_i(\vec{r})\cdot\vec{J}_d(\vec{r},t)d^3\vec{r} \\ &= -\int_S \Phi_i(\vec{r})\cdot\vec{J}(\vec{r},t)d\vec{s} = -I_i(t).\end{aligned} \tag{2}$$

The total current density $\vec{J}(\vec{r},t) = \vec{J}_c(\vec{r},t) + \vec{J}_d(\vec{r},t)$ is composed of conduction $\vec{J}_c(\vec{r},t)$ plus displacement $\vec{J}_d(\vec{r},t)$ components, where $\vec{\nabla}\cdot\vec{J}(\vec{r},t) = 0$. The actual electric field present inside the system, $\vec{E}(\vec{r},t)$, computed from the classical set of Maxwell equations,[22] is defined from the scalar potential $A_0(\vec{r},t)$ and also from a vector potential $\vec{A}(\vec{r},t)$ via $\vec{E}(\vec{r},t) = -\vec{\nabla}A_0(\vec{r},t) - \partial\vec{A}(\vec{r},t)/\partial t$. Thus, the displacement current is equal to $\vec{J}_d(\vec{r},t) = -\varepsilon(\vec{r})(\partial/\partial t)\vec{\nabla}[A_0(\vec{r},t)] - \varepsilon(\vec{r})\partial^2\vec{A}(\vec{r},t)/\partial t^2$. Therefore, the integral for the displacement current in Eq. (2) can be rewritten as

$$\int_{\Omega} \vec{F}_i(\vec{r}) \cdot \vec{J}_d(\vec{r},t) d^3\vec{r} = -\int_{\Omega} \vec{F}_i(\vec{r}) \varepsilon(\vec{r}) \frac{\partial}{\partial t} \vec{\nabla}[A_0(\vec{r},t)] d^3\vec{r} - \int_{\Omega} \vec{F}_i(\vec{r}) \cdot \frac{\partial^2 \vec{A}(\vec{r},t)}{\partial t^2} d^3\vec{r}. \quad (3)$$

The first volume integral in the right-hand side can be simplified to a surface integral $\int_{\Omega} \vec{F}_i(\vec{r}) \varepsilon(\vec{r}) (\partial/\partial t) \vec{\nabla}[A_0(\vec{r},t)] d^3\vec{r} = \int_S \vec{F}_i(\vec{r}) \varepsilon(\vec{r}) (\partial/\partial t) A_0(\vec{r},t) d\vec{s}$ by using the vector identity

$$\vec{\nabla}\left(\vec{F}_i(\vec{r}) \varepsilon(\vec{r}) \frac{\partial}{\partial t} A_0(\vec{r},t) \right) = \vec{F}_i(\vec{r}) \varepsilon(\vec{r}) \cdot \vec{\nabla}\left(\frac{\partial}{\partial t} A_0(\vec{r},t) \right) + \frac{\partial}{\partial t} A_0(\vec{r},t) \vec{\nabla}[\vec{F}_i(\vec{r}) \varepsilon(\vec{r})] \quad (4)$$

where the second term in the right-hand side of Eq. (4) is zero because of expression (1). Therefore, introducing the results (3) and (4) into (2), the total time-dependent current through the surface S_i is

$$I_i(t) = \Gamma_i^q(t) + \Gamma_i^e(t) + \Gamma_i^m(t), \quad (5a)$$

$$\Gamma_i^q(t) = -\int_{\Omega} \vec{F}_i(\vec{r}) \cdot \vec{J}_c(\vec{r},t) d^3\vec{r}, \quad (5b)$$

$$\Gamma_i^e(t) = \int_S \vec{F}_i(\vec{r}) \varepsilon(\vec{r}) \frac{\partial}{\partial t} A_0(\vec{r},t) d\vec{s}, \quad (5c)$$

$$\Gamma_i^m(t) = \int_{\Omega} \vec{F}_i(\vec{r}) \cdot \frac{\partial^2 \vec{A}(\vec{r},t)}{\partial t^2} d^3\vec{r}. \quad (5d)$$

We use the subscript i in expression (5) because the current through a surface different from S_i leads to a different definition of $\vec{F}_i(\vec{r})$. In principle, the computation of the time-dependent current needs a self-consistent scheme. For quantum computations, the knowledge of $\vec{J}_c(\vec{r},t)$ is obtained from the many-particle wave function (solution of the Schrödinger equation), once the scalar potential $A_0(\vec{r},t)$ and the vector potential $\vec{A}(\vec{r},t)$ are known. In order to close the self-consistent loop, such potentials have to be obtained from Maxwell equations using the appropriate charge distribution and particle current density (obtained from the wave function). In any case, any practical computation of expression (5) needs some simplifying assumptions.

B. Simplifying assumptions

In most practical conditions, the term $\Gamma_i^m(t)$ [expression (5d)] can be neglected compared to the other two terms. A "quasielectrostatic" approximation, $\vec{E}(\vec{r},t) \approx -\vec{\nabla} A_0(\vec{r},t)$, can be adopted[25,26] for nanometric dimensions at frequencies lower than a few terahertz. It can be shown that the role of $\vec{A}(\vec{r},t)$ in expression (5) can be neglected compared to the role of $A_0(\vec{r},t)$ when the device size L is much smaller than the minimum wavelength of the electromagnetic field $\lambda = c/f \gg L$, where c is the electromagnetic propagation speed and f is the signal oscillating frequency [see expression (2.30) in Ref. 26]. For the dimensions used in this work, shorter than 0.1 μm, the electromagnetic vector potential can be reasonably neglected at frequencies lower than about 50 THz. The term $\Gamma_i^m(t)$ has to be considered when the propagation of electromagnetic energy through the system becomes meaningful.[38]

On the other hand, the term $\Gamma_i^e(t)$ [expression (5c)] can be evaluated without taking into account the self-consistent loop. The first term $\Gamma_i^q(t)$ [expression (5b)] integrates the conduction current density inside the whole volume Ω, but this second term $\Gamma_i^e(t)$ integrates the scalar potential only over the whole surface S. Since most of the scalar potentials on the surfaces S_i are determined by the external bias, we can reasonably assume that the scalar potential at the boundaries, $A_0(\vec{r},t)$, $\vec{r} \in S$, is independent of the electron dynamics. Therefore, this term $\Gamma_i^e(t)$ depends only on the particular three-dimensional (3D) surface geometry of the device, the permittivity, and the temporal variations of the external bias. For simplicity, in this work we will assume that the device geometry makes the value of the term (5c) negligible in comparison with the term (5b). In any case, the term $\Gamma_i^e(t)$ can be computed "classically" once the particular 3D geometry of the device is specified and it can be added to the numerical results presented here.

Finally, in order to provide an analytical expression for the function $\vec{F}_i(\vec{r})$ and simplify our discussion, we consider the particular parallelepiped drawn in Fig. 2. The transport dimension (from source to drain) is much smaller than the other two dimensions, $L_x \ll L_y, L_z$. We define the function $\vec{F}_1(\vec{r})$ through the particular boundary conditions $\Phi_1(\vec{r}) = 1, \vec{r} \in S_1$, and $\Phi_1(\vec{r}) = 0, \vec{r} \in S_{h \neq 1}$. Under these conditions, it can be easily shown that the vector function $\vec{F}_1(\vec{r})$ can be approximated by a constant electric field[39] pointing from drain to source, $\vec{F}_1(\vec{r}) = -(1/L_x)\vec{x}$, where $|\vec{x}| = 1$. Since the x dimension is the only significant device length, we define $L = L_x$. Therefore, in the particular geometry of Fig. 2, only the x component of the conduction current density, $J_c(\vec{r},t)|_x$, is needed to evaluate the time-dependent quantum current:

$$I(t) = -\int_{\Omega} \vec{F}_1(\vec{r}) \cdot \vec{J}_c(\vec{r},t) d^3\vec{r} = \frac{1}{L} \int_{\Omega} J_c(\vec{r},t)|_x d^3\vec{r}. \quad (6)$$

For simplicity, we name the total current $I_i(t)$ through the S_1 surface as $I(t) = I_1(t)$. Arbitrary device geometries (different from the particular parallelepiped drawn in Fig. 2) only need a careful evaluation of the vector function $\vec{F}_1(\vec{r})$ and its effect on the integrals in (5).

C. The conduction and the displacement currents

In the previous section, we showed that the total current through S_1 can be equivalently computed from its original definition [from a surface integral of the total current density, $\vec{J}(\vec{r},t) = \vec{J}_c(\vec{r},t) + \vec{J}_d(\vec{r},t)$, evaluated at $\vec{r} \in S_1$] or from expression (5). Let us discuss the differences between the compu-

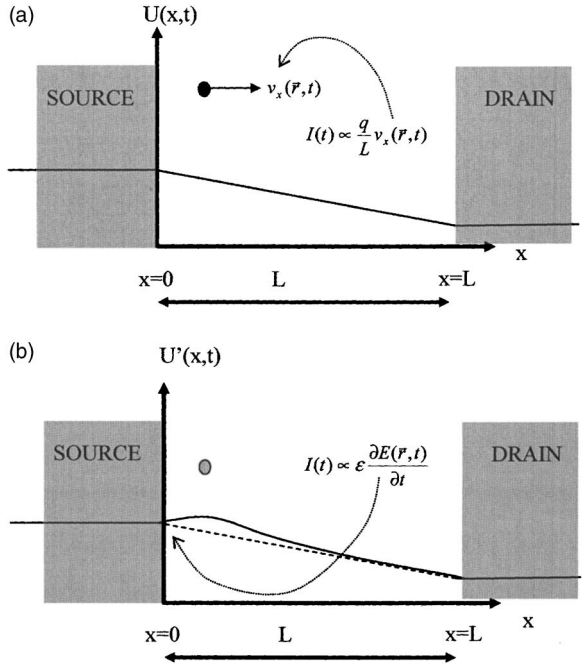

FIG. 3. Schematic representation of the time-dependent current associated with a single electron crossing the device active region. (a) The internal displacement current, associated with the electron movement, is obtained from the electron dynamics computed using the potential energy $U(x,t)$ due to the external bias. (b) This displacement current can be computed also from the time derivative of the electric field generated by the electron on the S_1 surface (defined here at x=0). The electric field is computed from the potential energy $U'(x,t)$ due to the external bias and the charge of this electron. The Ramo-Shockley theorem shows that both procedures are equivalent.

tational procedure of both expressions for a simple example: a single particle traversing a one–dimensional (1D) potential (see Fig. 3). The computation of the current following the elemental definition $\vec{J}(\vec{r},t)=\vec{J}_c(\vec{r},t)+\vec{J}_d(\vec{r},t)$ needs a two-step procedure. First, the conduction current (i.e., the electron dynamics) has to be computed from the Schrödinger and Maxwell equations using the potential energy profile $U(x,t)$ as seen in Fig. 3(a) (the electron does not interact with itself). Second, the displacement current (temporal variations of the electric field at S_1) has to be obtained by solving a new set of Maxwell equations (including now the charge of this electron) using the potential energy profile $U'(x,t)$ as seen in Fig. 3(b). On the contrary, the Ramo-Shockley theorem[25,26] only needs the first step to compute the total current. The second step is implicitly included in the development leading to expression (5). In summary, once the electron dynamics are known, the Ramo-Shockley theorem provides an accurate evaluation of the experimental current.[22–26]

The displacement current is mainly contained in the term (5c), but also in the term (5b), as we show below. We divide the displacement current into an external component related to $\Gamma_i^e(t)$ and an internal component related to $\Gamma_i^q(t)$. We consider again the simple example drawn in Fig. 3. The well-known "classical" expression of the Ramo-Shockley theorem,[22–24] $I(t)=(q/L)v_x(\vec{r},t)$, can be recovered from expression (6) when the current density is defined as $J_c(\vec{r},t)|_x = q v_x(\vec{r},t)[\delta(\vec{r}-\vec{r}(t))]$ where $\vec{r}(t)$ is the particle trajectory, q its electric charge, and $v_x(\vec{r},t)$ its velocity. An electron crossing the device generates a pulse in the macroscopic current $I(t)$, with a temporal length equal to the electron transit time and a height $(q/L)v_x(\vec{r},t)$. The current is different from zero even when the electron (or a localized wave packet inside the system) is not crossing the surface S_1. The pulse in $I(t)$ is related to the displacement current originated on the surface S_1 due to the temporal variations of the electric field generated by the movement of the electron charge inside the system (the potential can be fixed at the boundaries, but not its spatial derivate, i.e., the electric field). This internal component of the displacement current does not disappear even under dc conditions. This phenomenology is well understood when the Ramo-Shockley theorem is applied in other fields, for example, in classical Monte Carlo[40] analysis of electron transport. The rest of the displacement current, the external component (related to the temporal variation of the external bias), is contained in $\Gamma_e^i(t)$ and it is not explicitly computed in this work.

Let us mention that our previous argumentation about the role of the displacement and conduction currents can be extended to quantum systems using the de Broglie–Bohm approach.[41–44] Such quantum formalism provides an accurate description of quantum phenomenology in terms of well-defined quantum trajectories. The classical Ramo-Shockley theorem[23,24] (i.e., in terms of velocities) can be applied to a quantum system (i.e., in terms of current densities) by using the Bohm velocity, defined as $v_x(\vec{r},t)= J_c(\vec{r},t)|_x/|\Psi(\vec{r},t)|^2$ as outlined in Ref. 45.

III. QUANTUM CURRENT UNDER ARBITRARILY TIME-DEPENDENT POTENTIALS

In this work, we use expression (6) to compute the total time-dependent current for a quantum system. Here, we describe the computation of the conduction current density $J_c(\vec{r},t)|_x$ in a quantum scenario.

A. Independent-electron approximation

In principle, the quantum conduction current density should be computed from a wave-packet solution of the many-particle Schrödinger equation. The numerical difficulties in solving the many-particle wave function frustrate this possibility.[46] The potential profile of such a Hamiltonian would contain time-dependent terms corresponding to the electrostatic potential due to the applied external voltages (determined by the Coulomb interaction between the electrons inside the system and those in the gates or source or drain contacts) plus electron-electron terms due to the Coulomb interaction among the electrons inside the system. The procedure to compute the quantum current density can be greatly simplified if we assume that the potential profile is mainly determined by the external bias, and that the electron-electron terms have a negligible influence on it. Then, the potential becomes separable and we deal with single-particle Schrödinger equations. We introduce the words "independent

electrons" in the title of this paper to recognize this approximation. In fact, most time-dependent electron transport theories for open systems found in the literature[3,6,9,10,28,30] (with few exceptions[11–15]) do not take into account the electron-electron Coulomb interaction.[47]

We want to clarify the meaning of our approximation of independent electrons within the Ramo-Shockley theorem. We assume that electron dynamics is mainly determined by the external voltage (in fact, transistors are deliberately designed to provide exclusive gate control over the source-drain conductance). Then, as described in Fig. 3, each electron moving inside the system generates a conduction current and an internal displacement current, which are accurately considered in the expression (6) for our single-particle formalism. Our independent-electron formalism assumes that the electrons keep roughly the same motions that they had when considered independently. Obviously, the present approximation cannot be applied to systems where transport is determined by Coulomb blockade phenomenology.[48]

Now, we discuss the fulfillment of the particle continuity equation within our approach. The Schrödinger equation (even for noninteracting electrons under time-dependent potentials) includes a charge continuity equation (see Ref. 49). In our approach, the internal displacement current computed through expression (6) is related to the temporal derivative of electron probability (assumed as the electron density). In addition, another charge continuity equation appears if Maxwell equations are taken into account (see Ref. 50). Therefore, our approach does accomplish a particle continuity equation (due to the Schrödinger equation), but this does not guarantee that the Maxwell continuity equation, which needs a self-consistent loop, is also satisfied. Our approximation assumes that the two terms of the "Schrödinger" continuity equation $\partial\rho'/\partial t$ and $\vec{\nabla}\cdot\vec{J}_c'$ (obtained for independent electrons) are quite comparable to the two terms of the "Maxwell" continuity equation $\partial\rho/\partial t$ and $\vec{\nabla}\cdot\vec{J}_c$. As we have mentioned, this assumption is valid when the Coulomb blockade phenomenology and electromagnetic radiation can be neglected.

B. Quantum current for a flux of independent electrons

The total conduction current density in expression (6) for independent electrons is equal to the sum of the single-particle current densities $J_c^j(\vec{r},t)|_x$. The superindex j refers to the current density of the jth electron. For N electrons inside the volume Ω, we obtain

$$J_c(\vec{r},t)|_x = q\sum_{j=1}^{N} J_c^j(\vec{r},t)|_x \tag{7}$$

where we explicitly write the electron charge q in Eq. (7) because we use the standard Schrödinger particle current density [see Eq. (B15)] instead of the charge current density. In order to discuss our approach in a simple scenario, we assume that the 3D wave function can be written as a product of 1D wave functions. In the transport direction, the Hamiltonian that describes each electron is

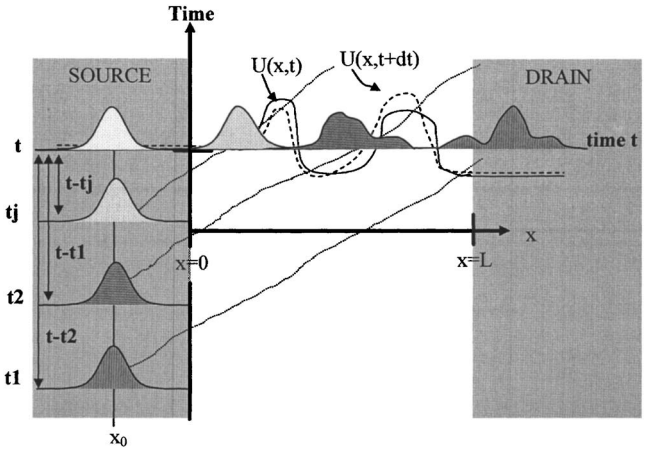

FIG. 4. Schematic time evolution of four different wave packets with different injection times. Each wave packet evolves during the time $t-t_j$ (from its particular initial time t_j to the global final time t). Since the potential energy $U(x,t)$ is different from $U(x,t+dt)$, each particular wave packet "sees" its own time-dependent potential energy profile.

$$\hat{H} = -\frac{\hbar^2}{2m}\frac{\partial^2}{\partial x^2} + U(x,t) \tag{8}$$

where m is the electron effective mass. We do not consider any relativistic effect or spin-orbit interaction. The second term of the Hamiltonian is the potential energy $U(x,t)$, which can vary arbitrarily (even temporal discontinuities leading to transient currents in quantum systems), as seen in Fig. 4. The average energy of a wave function evolving under $U(x,t)$ is not a constant of motion.[51] Hence, the quantum transport process cannot be described using energy eigenstates.[52] In addition, the standard Floquet states[3–6] are not valid for the nonperiodic Hamiltonian discussed here. In our approach, the wave functions are obtained directly from the numerical solution of the time-dependent Schrödinger equation with time-dependent potentials. As initial conditions, we use square integrable wave functions defined by an initial Gaussian wave packet (see Ref. 53 and the appendixes for details).

The rest of the subsection is devoted to evaluating the sum in expression (7). In this work, electron transport is modeled as a constant flux of time-dependent wave packets. We suppose that all electrons are described by wave packets with the same central energy E (i.e., we consider a narrow energy interval) injected from the source. Later, we will generalize the results to all possible central energies. Thus, all initial wave packets have identical descriptions, except for an offset in its time evolution (see Fig. 4). We define t_j as the time when the j wave packet presents its minimum position-momentum uncertainty. This initial time will be a useful label for the wave packets $\Psi_{t_j}^S(x,t)$ where the subscript t_j refers to the initial time and the superscript S refers to injection from the source. If we assume that the temporal separation between consecutive wave packets tends to zero (i.e., a large number of electrons traverse the device with $L_y, L_z \gg L_x$ in Fig. 2), the sum over all wave packets in Eq. (7) can be interpreted as an integral over the current density (which

does only depend on the x direction) of all t_j wave packets $J^S_{t_j}(x,t)$ injected from the source:

$$J_c(x,t)|_x = C'q\int_{t_j=-\infty}^{t} dt_j\, J^S_{t_j}(x,t). \tag{9}$$

The constant C' takes into account the injection rates.[54] Here, the wave packets with initial time $t_j \geqslant t$ do not contribute to the time-dependent current $I(t)$ because their presence probability inside the device, at this time t, is zero, as seen in Fig. 4. In other words, we have to consider only injection times $-\infty \leqslant t_j \leqslant t$. When expression (9) is introduced into (6), we conclude that the quantum time-dependent current, at time t, for a flux of electrons injected with central energy E from the source is equal to

$$I^S_E(t) = \frac{1}{L}\int_{x=0}^{L} dx \int_{S_1} dy\, dz\, J_{cx}(x,t)$$

$$= C\frac{q}{L}\int_{t_j=-\infty}^{t} dt_j \int_{x=0}^{L} dx J^S_{t_j}(x,t). \tag{10}$$

The constant C takes into account the role of the surface S_1 and the injection rates.[54] The superscript S means source injection and the subscript E indicates that the wave packet energies belong to a narrow energy interval around this value (see Appendix B for the definition of the wave packet). The right hand-side of expression (10) is the main result of this work. As we will show later, the generalization of expression (10) to all energies can be obtained by just summing the quasimonoenergetic contributions over all possible central energies. Let us emphasize that we are considering an "infinite" number of electrons traversing the system distributed over all wave packets and positions. Then, expression (10) is not valid for studying few electrons or current noise phenomenology (preliminary works in this direction can be found in Refs. 48 and 55). Finally, let us recall that the conduction current and the internal component of the displacement current are directly included in expression (10). In addition, the complete role of the potentials $A_0(\vec{r},t)$ and $\vec{A}(\vec{r},t)$ can be explicitly taken into account in our approach, if needed, by computing the terms (5c) and (5d).

C. The quantum current coefficient

In order to provide a better understanding of expression (10), we provide a compact notation to discuss its meaning. We define two parameters $D^S(E,t)$ and $D^D(E,t)$ as

$$D^{S/D}(E,t) = \frac{1}{L}\int_{t_j=-\infty}^{t} dt_j \int_{x=0}^{L} dx\, J^{S/D}_{t_j}(x,t) \tag{11}$$

where the superindex S/D means injection from the source/drain contact (see Fig. 5). Let us notice that $D^{S/D}(E,t)$ are unitless magnitudes that specifically depend on the electron injection energy E and the time t. Then, expression (10) is simply evaluated as $I^S_E(t) = qC[D^S(E,t)]$. The role of $D^S(E,t)$ is similar to the role of the transmission coefficient under dc conditions. We name this parameter the *quantum current coefficient*. In order to compare our approach with the scattering matrix formalism in the energy domain, let us emphasize that the quantum current coefficient depends on the injection energy E of electrons, but it also includes a broad range of possible final electron energies E'. In other words, it contains the inelastic transport processes from a particular initial energy E to all possible final energies E'.

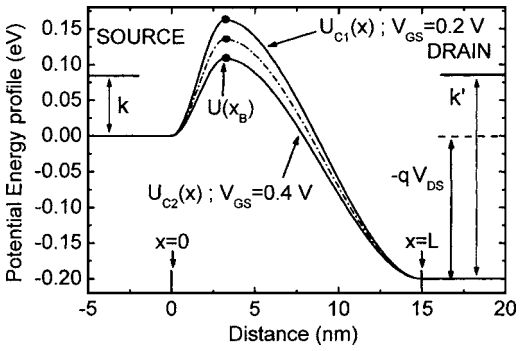

FIG. 5. Potential energy profile for a simple 1D transistor model with the bias condition described in Fig. 1. The profile depends on time inside the device active region ($0 \leqslant x \leqslant L$) and is constant outside. The potential energy profile $U(x,t)$ is controlled by the time-dependent gate bias and it changes continuously from $U_{C2}(x)$ to $U_{C1}(x)$.

Now, we compare the expression $D^S(E,t)$ with the well-known quantum transmission coefficient. The transmission coefficient for a wave packet injected from the source S with central energy E, $T^S(E)$, can be defined as the total electron presence probability at the right of the device active region ($x > L$ in Fig. 5), when the electron interaction with the barrier has finished:[53]

$$T^S(E) = \int_{x=L}^{x=\infty} |\Psi^S(x, t\to\infty)|^2 dx \equiv \int_{t=0}^{t=\infty} J^S(x_l,t)dt. \tag{12}$$

An initial wave packet $\Psi^S(x,0)$ is defined, at time $t=0$, located at x_0 deep inside the source (the injection time is not explicitly written). As shown in the right-hand side of expression (12), the $T^S(E)$ can also be computed from the temporal integral of $J^S(x_l,t)$ due to the Schrödinger particle conservation law. Since $T^S(E)$ is not dependent on the particular position x_l where the current is evaluated,[53] we can introduce the useless integral $(1/L)\int_{x_l=0}^{x_l=L} dx_l$ in the right-hand side of expression (12). Then, we can rewrite $T^S(E) = (1/L)\int_{x_l=0}^{x_l=L} dx_l \int_{t=0}^{t=\infty} J^S(x_l,t)dt$. As we will see in Sec. V, we can expect that the numerical values of expressions (11) and (12) are quite comparable because the temporal intervals where the current is meaningful are also comparable (inside the spatial region $0 \leqslant x \leqslant L$).

Now, let us explain the differences between $T^S(E)$ and $D^S(E,t)$. These differences imply that the generalization of the Landauer approach to time-dependent scenarios cannot rely on the transmission coefficient. In particular, we discuss the role played by the initial central position of the wave packet, x_0, in expressions (11) and (12). The transmission coefficient for a wave packet in static potentials is independent on such an initial position (see Appendix B), but $T^S(E)$

drastically depends on this arbitrary position when time-dependent potentials are considered (see Ref. 56 for a particular example). Such arbitrary dependence of the results on the initial position disappears when computing $D^S(E,t)$. For the latter, changing the initial central position of a wave packet can be related to the changing of the initial time t_j (see Ref. 57). Since expression (11) is computed from an infinite number of initial times, such temporal offset is completely irrelevant in the computation of $D^S(E,t)$. Therefore, the computation of the time-dependent quantum current is related to the quantum current coefficient, and not to the quantum transmission coefficient.

The generalization of the expression (10) to all possible central energies can be obtained by summing the quasimonoenergetic current contribution over all energies weighted by the occupation function of each contact. We consider injection from the drain and source contacts. Thus,

$$I(t) = q\int_{E=0}^{\infty} g(E)\{D^S(E,t)f^S(E) - D^D(E,t)f^D(E)\}dE \tag{13}$$

where $g(E)$ is the density of states that contains the previous C constant for each energy.[58] We deal with ideal source and drain reservoirs. We define $f^S(E)$ and $f^D(E)$ as the Fermi-Dirac function at the source and drain contacts, respectively:

$$f^{\alpha}(E) = \frac{1}{1+\exp[(E+E_{\perp}-E_{F\alpha})/k_BT]}, \quad \alpha = S,D, \tag{14}$$

where k_BT is the thermal energy and $E_{\perp}$ is the energy in the lateral directions. We have defined two pseudoequilibrium Fermi levels, E_{FS} and E_{FD}, at the source and drain contacts respectively, whose difference is proportional to the applied source-to-drain voltage.

IV. QUANTUM CURRENT UNDER STATIC POTENTIALS

In the previous section we have shown that the quantum transmission coefficient has to be substituted by the quantum current coefficient for the computation of the current in time-dependent scenarios. Here, we show that both coefficients are identical when static potentials are considered. In other words, we show that the quantum time-dependent current in Eq. (13) directly leads to the well-known Landauer dc current[59,60] when static potentials are considered. The equivalence between both models can be established by showing that $D^S(E,t)|_{static} = D^D(E,t)|_{static} = T(E)|_{static}$ for each energy E.

Let us focus on electrons injected from the source with central energy E. For static potential profiles, the time evolution of all wave packets used in the computation of (10) can be defined according to a unique wave packet $\Psi^S(x,t)$ injected at time $t=0$. The time evolution of any other wave packet $\Psi_j^S(x,t)$ injected at the particular initial time t_j can be related to the former by $\Psi_j^S(x,t)=\Psi^S(x,t-t_j)$. Both wave packets always "feel" the same static potential (this is not true for time-dependent potentials). Then, expression (11) can be rewritten as

$$D^S(E,t)|_{static} = \frac{1}{L}\int_{t_j=-\infty}^{t} dt_j \int_{x=0}^{L} dx\, J_{t_j}^S(x,t) = \frac{1}{L}\int_{t_j=-\infty}^{t} dt_j \int_{x=0}^{L} dx\, J^S(x,t-t_j). \tag{15}$$

Using the variable $t'=t-t_j$, the temporal integral of the current density can be rewritten as

$$D^S(E,t)|_{static} = \frac{1}{L}\int_{x=0}^{L} dx \int_{t\prime=0}^{t'=\infty} dt' J^S(x,t') = \frac{1}{L}\int_{x=0}^{L} dx\ T(E)|_{static} = T(E)|_{static} \tag{16}$$

where we have used definition (12) and the fact that $T(E)|_{static}$ is independent of the position x where the current density is evaluated.[53] Therefore, the identity $D^S(E,t)|_{static} = T(E)|_{static}$ holds. Following identical steps, it is found that $D^D(E,t)|_{static} = T(E)|_{static}$. We have not used the superscript S/D in $T(E)|_{static}$ because the transmission coefficient for a wave packet evolving in static potentials does not depend on the injection side (see Appendix B). Again, the generalization to all energies can be straightforwardly obtained by weighting $D^{S/D}(E,t)$ according to Fermi-Dirac statistics. Then, the Landauer approach[59,60] is exactly recovered from expression (13) when static potentials are considered.

V. NUMERICAL APPLICATIONS

Now, in order to show the numerical implementation of our formalism, we study a silicon double-gate field-effect transistor (DG-FET) driven under a nonperiodic external signal (see Fig. 5). We consider an intrinsic channel of $L=15$ nm length. The device lengths in the z and y directions are large enough to assume an infinite number of injected electrons from both sides. For simplicity, we assume a hand-made 1D potential profile inside the device, $U(x,t)$, whose shape directly depends on the gate voltage $V_{GS}(t)=V(t)$ as follows:

$$U(x,t) = \frac{Uc_1(x)+Uc_2(x)}{2} - \gamma(t)\frac{Uc_1(x)-Uc_2(x)}{2} \tag{17}$$

where the function $\gamma(t)$ is a unitless parameter that provides the profile of $U(x,t)$ by linear interpolation, as a function of the time-dependent gate variations $V(t)=V_{GS}(t)-0.3$ V. For the times t' when $\gamma(t')=-1$, we obtain $U(x,t')=Uc_1(x)$ which corresponds to non-self-consistent profile for $V_{GS}=0.2$ V and $V_{DS}=0.2$ V (as depicted in Fig. 5). For $\gamma(t'')=1$, we obtain $U(x,t'')=Uc_2(x)$ which corresponds to $V_{GS}=0.4$ V and $V_{DS}=0.2$ V (see Fig. 5). For a general time, in these particular bias conditions, we have $\gamma(t)=V(t)/0.1$ V.

The gate voltage variation signal $V(t)$ (i.e., the driving signal), is defined as a frequency modulation (FM) signal:

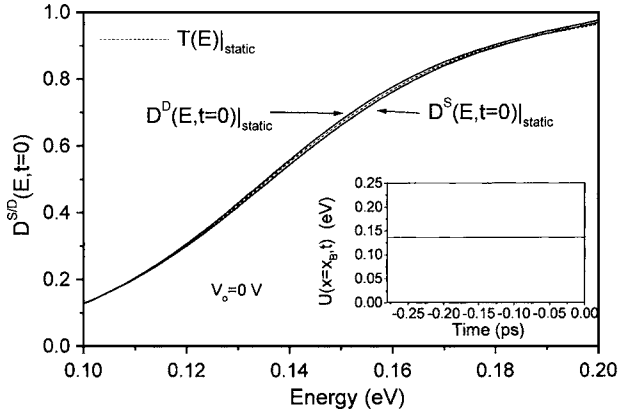

FIG. 6. Solid line, quantum current coefficient $D^{S/D}(E,t)$ for time $t=0$ as a function of energy for static conditions. Dotted line, static transmission coefficient. Inset: Time evolution of $U(x_B,t)$ for the position x_B defined in Fig. 5.

$$V(t) = V_0 \cos[w_c t + \beta \sin(w_m t)]$$
$$= V_0 \sum_{n=-\infty}^{n=\infty} J_n(\beta)\cos[(w_c + n w_m)t] \qquad (18)$$

where V_0 is the amplitude of the gate signal, w_c is the carrier frequency, w_m is the modulating frequency, β is the modulating index that determines the frequency spectrum of the FM signal, and, on the right-hand side, $J_n(\beta)$ is the first-class Bessel function.[61] We select the FM signal because it is a simple example of a quite common signal (in communication systems) that cannot be studied within the powerful Floquet formalism (because it is not periodic). Later, we will briefly discuss the ability of these phase-coherent devices to perform quantum demodulation at very high frequencies and other possible applications.

In Figs. 6–10, we have represented the computation of the quantum current coefficient at the particular time $t=0$ for different values of the driving signals (18). First of all, let us explain the numerical procedure for computing $D^{S/D}(E,t)$.

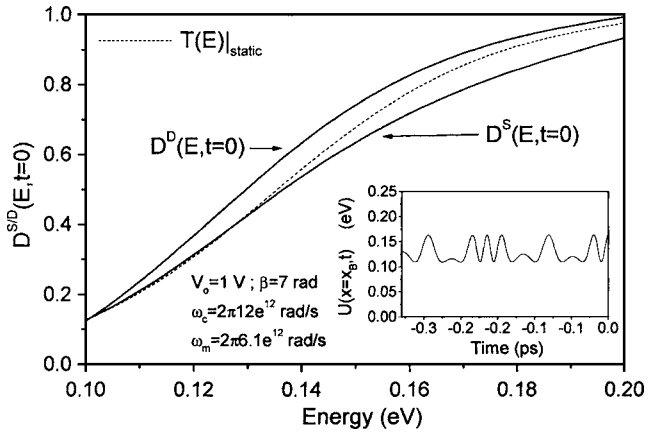

FIG. 7. Solid line, quantum current coefficient $D^{S/D}(E,t)$ for time $t=0$ as a function of energy for time-dependent conditions. Dotted line, static transmission coefficient. Inset: Time evolution of $U(x_B,t)$ for the position x_B defined in Fig. 5.

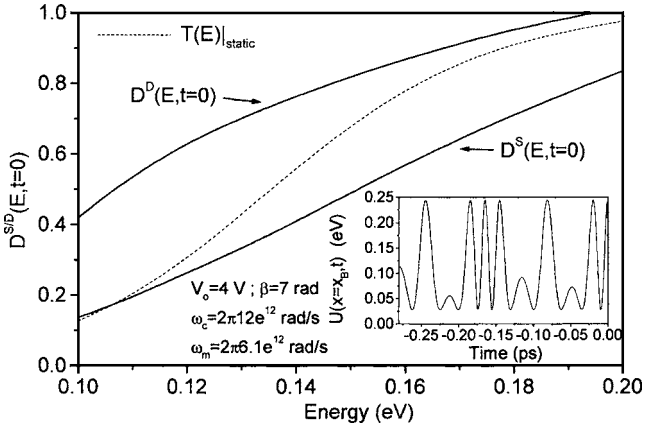

FIG. 8. Solid line, quantum current coefficient $D^{S/D}(E,t)$ for time $t=0$ as a function of energy for a gate signal amplitude higher than that in Fig. 7. Dotted line, static transmission coefficient. Inset: Time evolution of $U(x_B,t)$ for the position x_B defined in Fig. 5.

For each energy E, the time evolution of a large number of different wave packets has to be computed. A wave packet is defined by an initial Gaussian wave packet described by expressions (A5) and (A6). Its initial central position x_0 is situated far from the system to guarantee that the presence probability is negligible inside the device active region at the initial time t_j. In particular, we use $x_0=-70$ nm for source injection and 85 nm for drain injection. In both cases, we use initial spatial dispersions equal to $\sigma_x=30$ nm for all wave packets. We use wave packets much larger than the system $L=15$ nm to model injection of square-integrable quasimonoenergetic wave functions.[62,63] Then, the evolution of each j wave packet is determined from t_j until t by numerically solving the time-dependent Schrödinger equation (see the detailed procedure in Appendix A). Once we know the wave function at time t, we evaluate the quantum particle current density [Eq. (B15)] at all positions $0 \leqslant x \leqslant L$. All this procedure has to be repeated for each j wave packet with initial

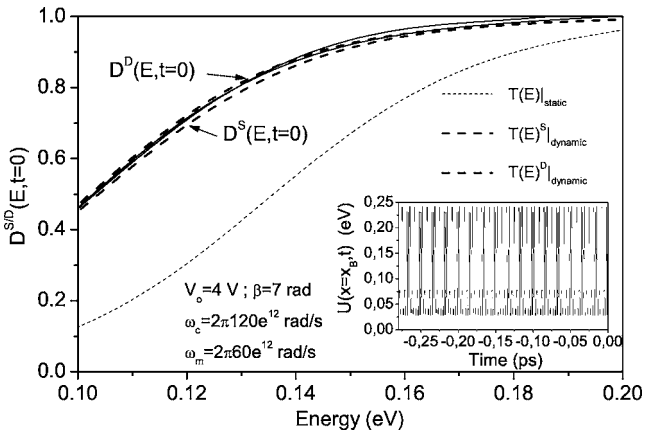

FIG. 9. Solid line, quantum current coefficient $D^{S/D}(E,t)$ for time $t=0$ as a function of energy. A periodic FM signal at the gate contact is considered with frequencies higher than those in Fig. 8. Dashed line, dynamic transmission coefficient; dotted line, static transmission coefficient (of Fig. 6). Inset: Time evolution of $U(x_B,t)$ for the position x_B defined in Fig. 5.

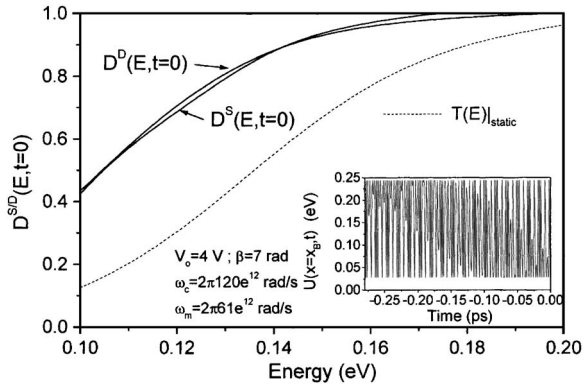

FIG. 10. Solid line, quantum current coefficient $D^{S/D}(E,t)$ for time $t=0$ as a function of energy. A nonperiodic FM signal at the gate contact is considered. Dotted line, static transmission coefficient. Inset: Time evolution of $U(x_B,t)$ for the position x_B defined in Fig. 5.

time $-\infty < t_j < t$ (see Ref. 64) to compute $D^{S/D}(E,t)$ from expression (11). Each j wave packet experiences a completely different potential profile $U(x,t)$ depending on its injection time (see Fig. 4). In order to compute the instantaneous current at time t, the whole procedure has to be repeated for wave packets injected from the source and drain contacts, and for the whole energy range.

In Fig. 6, we have used the parameter $V_0=0$ V in expression (18), so that the potential is static and equal to $U(x)=[Uc_1(x)+Uc_2(x)]/2$ (the dashed line in Fig. 5). The inset of Fig. 6 shows the constant value of the potential profile $U(x_B,t)$ at the position x_B defined in Fig. 5. Using expression (12), we have also plotted the transmission coefficient for the source or drain injection sides. As expected, and as is explicitly shown in Appendix B, the transmission coefficient $T(E)|_{static}$ computed from expression (12) is independent of the injection side. In addition, we clearly see that $D^S(E,t)|_{static} = D^D(E,t)|_{static} = T(E)|_{static}$. Hence, Fig. 6 is basically a numerical confirmation of the theoretical argumentation presented in Sec. IV. The small differences among the curves are due to spurious results of the numerical method.

In Fig. 7, we have repeated the same computation, but using the following values: $V_0=1$ V, $w_c=2\pi\times 12\times 10^{12}$ rad/s, $w_m=2\pi\times 6.1\times 10^{12}$ rad/s, and $\beta=7$ rad. Now, as expected, the values of $D^S(E,t)$ and $D^D(E,t)$ are not equal and their value is also different from the static value of the transmission coefficient computed in Fig. 6. At the particular time $t=0$, we obtain $D^S(E,t) < D^D(E,t)$. We have checked that the previous inequality can be reversed at other times. In Fig. 8, we have represented the same information for a larger amplitude of the gate voltage, $V_0=4$ V [see the value of $U(x_B,t)$ in the inset in Fig. 8]. The difference between $D^S(E,t)$ and $D^D(E,t)$ is larger. The present preliminary results seem to suggest that the coherent pumping effect can be maximized by proper (nonperiodic) tailoring of the driving signal. In both figures, we have not plotted the quantum transmission coefficient under time-dependent conditions, $T(E)|_{dynamic}$, because it depends arbitrarily on the initial position x_0 (or, equivalently, on initial time t_j) as we have carefully discussed in Sec. III.

In Fig. 9, we have selected higher frequencies with $w_c=2\pi\times 12\times 10^{13}$ rad/s and $w_m=2\pi\times 6\times 10^{13}$ rad/s. The rest of the parameters are identical to those of Fig. 8. For these particular conditions ($w_c=2w_m$), expression (18) becomes a periodic signal $T=2\pi/w_m=100/6$ fs (as seen in the inset of Fig. 9). Then, we can make use of the powerful Floquet theory and the results can be explained by using Gravila's argumentation.[8] In the high-frequency nonadiabatic limit (frequencies much higher than the inverse of the electron dwell time), an average temporal potential profile gives a good insight into the properties of the time-dependent system. In particular, the time-averaged potential profile can be defined as

$$U_{eff}(x) = \frac{1}{T}\int_{-T/2}^{T/2} U(x,t)dt. \tag{19}$$

Now, the transmission coefficient for this time-dependent potential, $T(E)|_{dynamic}$, is also independent of the injection side and equal to $D^S(E,t)$ and $D^D(E,t)$ [and different from $T(E)|_{static}$ computed in Fig. 6]. In particular, we obtain a higher transmission coefficient in the results of Fig. 9 than in those of Fig. 6, because a lower time-averaged potential profile is obtained in Fig. 9, $U_{eff}(x) < U(x) \equiv [Uc_1(x)+Uc_2(x)]/2$. A lower potential profile means higher current and higher values of $D^{S/D}(E,t)$. The current computed from expression (13) will be time independent because the parameters $D^S(E,t)$ and $D^D(E,t)$ are, now, independent of time.

Finally, in Fig. 10, we have selected frequencies similar (but not identical) to those of Fig. 9, $w_c=2\pi\times 12\times 10^{13}$ rad/s and $w_m=2\pi\times 6.1\times 10^{13}$ rad/s. The rest of the parameters are identical to those of Fig. 9. Now, the FM signal and, thus, the Hamiltonian of Eq. (8) are not periodic. As we see in the inset of Fig. 10, the values of the energy potential profile fluctuate around 0.05 eV for times close to $t=0$ ps and around 0.25 eV for times around $t=-0.25$ ps. Therefore, the quantum transmission coefficient (not drawn) will depend, again, on the initial time t_j (or the initial position x_0) even in this nonadiabatic high-frequency limit. On the contrary, since the computation of the quantum current coefficient involves all possible initial times, the parameters $D^S(E,t)$ and $D^D(E,t)$ give similar values. Again, the current computed from expression (13) will be time independent because the parameters $D^S(E,t)$ and $D^D(E,t)$ are independent of time. In fact, such rapid variations of the potential profile can be used to control the transport process, and to increase or slow down tunneling by any desired degree, or even to suppress it altogether, in a perfect coherent way.[9,10]

In this section, we have seen that the numerical implementation of our approach is quite simple and it can be applied to study completely arbitrary time-dependent scenarios. Regarding digital applications, for example, the model can be used to analyze the transient current response to square-step voltage-driven quantum transistors. For analog application, simple one-transistor signal demodulators can be envisaged since the source-drain current depends on the gate frequency (as we have seen in Figs. 7–9). The approach presented here can also be used to obtain information about the dynamics of electrons driven by chaotic signals. All this in-

formation can provide a fresh view on the old controversial issue of tunneling times.[65–67] Much more work is needed to explore all these possibilities mentioned here briefly. In summary, the present approach provides a very useful tool (using the time domain, complementary to other energy-domain formalisms) to better understand time-dependent tunneling phenomenology and to study practical high-frequency applications of phase-coherent devices.

VI. CONCLUSIONS

An expression for computing the instantaneous particle current in phase-coherent devices driven by arbitrarily time-dependent potentials is presented [expression (10)]. The role of the Maxwell equations in determining the instantaneous current in phase-coherent devices is discussed through the Ramo-Shockley theorem. We develop our approach in a wave packet time domain within the first-quantization formalism. We consider that the quantum current density is mainly determined by the external bias, and that the electron-electron term has a negligible influence on it (as most time-dependent electron transport theories do,[3,6,9,10,28,30] with few exceptions[11–15]). On the other hand, neither eigenstates (the average energy is not a constant of motion[51]) nor Floquet states (nonperiodic Hamiltonians) can be used to define the electron wave function in general time-dependent scenarios. Wave functions obtained directly from the numerical solution of the time-dependent Schrödinger equation (see Appendix A) are used in this work. In particular, we consider quasi-monoenergetic initial Gaussian wave packets as initial boundary conditions.[62,63] The role of the scalar $A_0(\vec{r},t)$ and vector $\vec{A}(\vec{r},t)$ potentials can be explicitly included in our approach through terms (5c) and (5d).

We have shown that the time-dependent conductance is not proportional to the quantum transmission coefficient, but to a parameter named the quantum current coefficient. As an important test, we showed that the time-dependent quantum current obtained with our approach directly leads to the well-known Landauer current[59,60] when static potentials are considered. As an example, the study of a simple 1D nanoscale DG-FET is presented.[27] The quantum current coefficient is computed for the DG-FET driven by a FM signal.[61] The FM signal is not periodic and the powerful Floquet formalism cannot be applied. The adiabatic and nonadiabatic limits are analyzed. The present preliminary results seem to suggest that the coherent pumping effect can be maximized by proper (nonperiodic) tailoring of the driving signal. Finally, we have mentioned some possible applications for future phase-coherent transistors: the evaluation of transient quantum current in digital applications, one-transistor signal demodulators, coherent transport in systems driven by chaotic signals, etc. In summary, the approach presented here provides a useful tool (in the time domain, complementary to other energy-domain formalisms) to provide a deeper understanding of the delicate time-dependent tunneling phenomenology. In addition, the approach has a simple numerical algorithm which can be applicable to study practical digital or analog high-frequency properties of phase-coherent nanoscale devices.

ACKNOWLEDGMENTS

The authors are really grateful to Olivier Vanbesien and Javier Mateos for stimulating discussion. This work has been partially supported by the Ministerio de Ciencia y Tecnología and FEDER through Project No. TIC2003-08213-C02-02.

APPENDIX A: SOLUTION OF THE 1D SCHRÖDINGER EQUATION UNDER ARBITRARILY TIME-DEPENDENT POTENTIALS

In this appendix, we present the finite-difference method used to find the time evolution of wave packets. We describe electrons by the wave function $\Psi(x,t)$ that is the solution of the following Schrödinger equation:

$$i\hbar\frac{\partial\Psi(x,t)}{\partial t}=\hat{H}\Psi(x,t)=\left[-\frac{\hbar^2}{2m}\frac{\partial^2}{\partial x^2}+U(x,t)\right]\Psi(x,t) \tag{A1}$$

where m is the electron effective mass. The simulated time is discretized in temporal steps dt. The simulated region is also discretized in spatial steps dx. Then, the temporal and spatial derivatives present in expression (A1) can be numerically approximated as

$$\frac{\partial\Psi(x,t)}{\partial t}=\frac{\Psi(x,t+dt)-\Psi(x,t-dt)}{2dt}, \tag{A2}$$

$$\frac{\partial^2\Psi(x,t)}{\partial x^2}=\frac{\Psi(x+dx,t)-2\Psi(x,t)+\Psi(x-dx,t)}{dx^2}. \tag{A3}$$

Inserting Eqs. (A2) and (A3) into (A1), we obtain the following recursive expression:

$$\Psi(x,t+dt)=\Psi(x,t-dt)+i\frac{\hbar dt}{dx^2m}\{\Psi(x+dx,t)-2\Psi(x,t)+\Psi(x-dx,t)\}-i\frac{2dt}{\hbar}U(x,t)\Psi(x,t). \tag{A4}$$

Once we know the wave function at particular times t and $t-dt$ for all spatial positions, $\Psi(x,t)$ and $\Psi(x,t-dt)$, we can compute the wave function at the next time $t+dt$, $\Psi(x,t+dt)$, using Eq. (A4). The iterative application of Eq. (A4) provides the whole time evolution of the wave packet. The simulation box must be large enough so that the whole wave packet is contained in it, at any time, to avoid spurious reflections at the simulation box limits.

The initial values of the wave packet are fixed at the two initial times t_j and t_j-dt. The central position of the initial wave packet is defined deep inside the contact region so that the presence probability of the wave function in the device active region is zero at the initial time t_j. We consider that the wave packet at time $t=t_j$ evolves in a flat potential region. In particular, we define the initial wave function as a time-dependent Gaussian wave packet[53]

$$\Psi(x,t)=\left(\frac{2a^2}{\pi}\right)^{1/4}\frac{e^{i\varphi}}{[a^4+4\hbar^2(t-t_j)^2/m^2]^{1/4}}e^{i[k_c(x-x_0)]}\exp\left(-\frac{[x-x_0-(\hbar k_c/m)(t-t_j)]^2}{a^2+2i\hbar(t-t_j)/m}\right) \tag{A5}$$

where a is the spatial dispersion of the wave packet, m the particle effective mass, x_0 the central position of the wave packet at the initial time t_j, k_c the central wave vector $k_c=\sqrt{2mE/\hbar^2}$ in the x direction related to the central energy E, and $\varphi=-\theta-\hbar k_C^2 t/(2m)$ with $\tan(2\theta)=2\hbar t/(ma^2)$ (see Ref. 53). In particular, at the initial time $t=t_j$, we obtain the simplified expression

$$\Psi(x,t)=\left(\frac{2}{\pi a^2}\right)^{1/4}e^{i[k_c(x-x_0)]}\exp\left(-\frac{(x-x_0)^2}{a^2}\right). \tag{A6}$$

We define the wave packet spatial dispersion $\sigma_x=a/\sqrt{2}$ and the wave packet width in the wave vector space as $\sigma_k=1/\sigma_x$. In this work we use the values defined in Ref. 62.

Our experience suggests that this iterative procedure provides accurate results (the norm of the wave packets is conserved with high precision) when dx is on the order of 1–2 Å and the temporal step dt is around 10^{-17} s. The successive application of expression (A4) for long simulation times, as long as 500 000 times dt, provides accurate results when checked with known analytical solutions.

APPENDIX B: SOURCE AND DRAIN TRANSMISSION COEFFICIENT UNDER STATIC CONDITIONS

We show that the transmission coefficient of wave packets does not depend on the injection side, when static potentials are considered. First, we consider Hamiltonian eigenstates. Second, we show that the transmission coefficient of wave packets is equal to the weighted sum of transmission coefficients of Hamiltonian eigenstates.

As depicted in Fig. 5, we define $U(x)=U_S$ for $x<0$ and $U(x)=U_D$ for $x>L$. One set of convenient solutions that form a complete orthogonal set of wave vectors is given by the (incoming) scattering states.[52] The wave function for electrons coming from the drain contact with energy E and wave vectors k'_D and k_D is

$$\varphi^D(x)=\frac{1}{\sqrt{2\pi}}\begin{cases}t(k_D)\exp(ik_Dx), & x<0,\\ \exp(ik'_Dx)+r(k'_D)\exp(-ik'_Dx), & x>L,\end{cases} \tag{B1}$$

where the wave vectors are defined (see Fig. 5) as

$$k'_D=-\sqrt{\frac{2m(E-U_D)}{\hbar^2}}\quad\text{and}\quad k_D=-\sqrt{\frac{2m(E-U_S)}{\hbar^2}}. \tag{B2}$$

The transmission and reflection coefficients of the electron coming from the drain are

$$T^D(E)=\frac{k_D}{k'_D}|t(k_D)|^2\quad\text{and}\quad R^D(E)=|r(k'_D)|^2. \tag{B3}$$

For a state coming from the source with the same energy E, we have

$$\varphi^S(x)=\frac{1}{\sqrt{2\pi}}\begin{cases}t(k'_S)\exp(ik'_Sx), & x>L,\\ \exp(ik_Sx)+r(k_S)\exp(-ik_Sx), & x<0.\end{cases} \tag{B4}$$

Now, the wave vectors are defined as

$$k'_S=\sqrt{\frac{2m(E-U_D)}{\hbar^2}}\quad\text{and}\quad k_S=\sqrt{\frac{2m(E-U_S)}{\hbar^2}}. \tag{B5}$$

The transmission and reflection coefficients of the electron coming from the source are

$$T^S(E)=\frac{k'_S}{k_S}|t(k'_S)|^2\quad\text{and}\quad R^S(E)=|r(k_S)|^2. \tag{B6}$$

Since we are dealing with states whose probabilities do not change with time, the current is uniform and it can be easily shown that

$$T^S(E)+R^S(E)=1\quad\text{and}\quad k_S[1-|r(k_S)|^2]=k'_S|t(k'_S)|^2. \tag{B7}$$

Alternatively, we can construct the eigenstate (B1) from the eigenstates (B4) and its complex conjugate. The time-reversal symmetry of the system assures that the complex conjugate wave function is also a solution of the Hamiltonian. Thus, using expression (B4), it is possible to show that

$$\frac{\varphi^{S^*}(x)}{t^*(k'_S)}-r^*(k_S)\frac{\varphi^S(x)}{t^*(k'_S)}=\frac{1}{\sqrt{2\pi}}\begin{cases}\dfrac{1-|r(k_S)|^2}{t^*(k'_S)}\exp(-ik_Sx), & x<0,\\ \exp(-ik'_Sx)-\dfrac{r^*(k_S)}{t^*(k'_S)}t(k_S)\exp(ik'_Sx), & x>L,\end{cases} \tag{B8}$$

where $\varphi^{S^*}(x)$ is the complex conjugate of $\varphi^S(x)$. Comparing expressions (B1) and (B8), we deduce that the transmission coefficient of the eigenstate coming from the drain, expression (B3), can be written as

$$T^D(E)=\frac{k_D}{k'_D}|t(k_D)|^2=\frac{k_D}{k'_D}\frac{[1-|r(k_S)|^2][1-|r(k_S)|^2]}{|t(k'_S)|^2}. \tag{B9}$$

Using expression (B7), and since $k_D/k'_D=k_S/k'_S$, we obtain

$$T^D(E)=1-|r(k_S)|^2 \tag{B10}$$

and, from Eqs. (B3), (B6), and (B7), we can easily find

$$T^D(E)=\frac{k_D}{k'_D}|t(k_D)|^2=\frac{k'_S}{k_S}|t(k'_S)|^2=T^S(E). \tag{B11}$$

We have shown that the transmission coefficient of an eigenstate injected from the source is identical to the trans-

mission coefficient of an eigenstate, with the same total energy, injected from the drain.

Now, we use Eq. (B11) to show that the same conclusion can be extended to the quantum transmission coefficients of a wave packet. It is well known that any linear combination of Hamiltonian eigenstates $\varphi(x)$ is also a solution of the time-dependent Schrödinger equation with static potentials because of the superposition principle of quantum theory.[53] In order to simplify the notation, we assume that the wave packet is constructed from eigenstates coming from the source:

$$\Psi^S(x,t) = \int_0^{+\infty} dk_S a^S(k_S)\varphi^S(x)e^{-iEt/\hbar} \tag{B12}$$

where $a^S(k_S)$ is a complex quantity that must be sufficiently regular to allow differentiation inside the integral [for simplicity, we assume $a^S(k_S)=0$ for $k_S \leqslant 0$]. The energy is defined in the source contact as $E=\hbar^2 k_S^2/2m=\hbar w$. Using the closure relation, the value $a^S(k_S)$ is

$$a^S(k_S) = \int_{-\infty}^{\infty} dx\, \Psi^S(x,0)\varphi^{S^*}(x), \tag{B13}$$

which defines the wave packet in the k space. The transmission coefficient of a wave packet can be computed from the expression (12) in the text which we rewrite here:

$$T^S(E) = \int_{x=L}^{x=\infty} |\Psi^S(x,t\to\infty)|^2 dx \equiv \int_{t=0}^{t=\infty} J^S(x_l,t)dt. \tag{B14}$$

In particular, we use the right-hand side of expression (B14) to compute the transmission coefficient at $x_l > L$ (see Fig. 5) because the analytical expression of the Hamiltonian eigenstates, $\varphi^S(x)=1/\sqrt{2\pi}t(k'_S)\exp(ik'_S)$, is known. The current is evaluated according to

$$J(x,t) = -i\frac{\hbar}{2m}\left[\Psi^*(x,t)\frac{\partial\Psi(x,t)}{\partial x} - \Psi(x,t)\frac{\partial\Psi^*(x,t)}{\partial x}\right] \tag{B15}$$

where $\Psi^*(x,t)$ is the complex conjugate of $\Psi(x,t)$. It is quite easy to show that

$$T^S(E) = \frac{\hbar}{m}\frac{1}{2\pi}\int_{t=0}^{t=\infty} dt \int_{-\infty}^{\infty} dk_{S1}\int_{-\infty}^{\infty} dk_{S2}k'_{S1}a^S(k_{S1})t(k'_{S1})$$
$$a^{*S}(k_{S2})t^*(k'_{S2})e^{i(k'_{S2}-k'_{S1})x}e^{-i(w_1-w_2)t}. \tag{B16}$$

Using the following δ function definition:

$$\frac{1}{2\pi}\int_{t=0}^{t=\infty} dt\, e^{-i(w_1-w_2)t} = \frac{m}{\hbar}\frac{1}{k_{S2}}\delta(k_{S2}-k_{S1}), \tag{B17}$$

we obtain $k_{S2}=k_{S1}\equiv k_S$ and, therefore, $k'_{S2}=k'_{S1}\equiv k'_S$. Then, the final expression for the transmission coefficient is

$$T^S(E) = \int_{-\infty}^{\infty} dk_S |a^S(k_S)|^2 \frac{k'_S}{k_S}|t(k'_S)|^2. \tag{B18}$$

The evaluation of $T^D(E)$ follows identical steps and gives

$$T^D(E) = \int_{-\infty}^{\infty} dk'_D |a^D(k'_D)|^2 \frac{k_D}{k'_D}|t(k_D)|^2. \tag{B19}$$

Therefore, using expression (B11), the conclusion about the transmission coefficient of Hamiltonian eigenstates can be directly extrapolated to wave packets. We assume that the wave packets at each contact have identical definition in the wave-vector space, $|a^D(k'_D)|=|a^S(k_S)|$. Hence, Eqs. (B18) and (B19) show that the transmission coefficients of wave packets with total energy E evolving in static potentials do not depend on the injection side.

*Corresponding author. Email address: Xavier.Oriols@uab.es

[1] G. Platero and R. Aguado, Phys. Rep. **395**, 1 (2004).
[2] M. Buttiker and T. Christen, in *Mesoscopic Electron Transport*, edited by L. Kowenhoven, G. Schoen, and L. Sohn, NATO Advanced Studies Institute, Ser. E: Applied Science Series E, (Kluwer, Dordrecht, 1997).
[3] M. Grifoni and P. Hanggi, Phys. Rep. **304**, 229 (1998).
[4] U. Peskin and N. Moiseyev, Phys. Rev. A **49**, 3712 (1994).
[5] W. Li and L. E. Reichl, Phys. Rev. B **60**, 15732 (1999).
[6] M. Moskalets and M. Buttiker, Phys. Rev. B **66**, 205320 (2002).
[7] J. C. Wells, I. Simbotin, and M. Gavrila, Phys. Rev. A **56**, 3961 (1997).
[8] M. Gavrila and J. Z. Kaminski Phys. Rev. Lett. **52**, 613 (1985).
[9] F. Grossmann, T. Dittrich, P. Jung, and P. Hänggi, Phys. Rev. Lett. **67**, 516 (1991).
[10] I. Vorobeichik, R. Lefebre, and N. Moiseyev, Europhys. Lett. **41**, 111 (1998).
[11] A. Pretre, H. Thomas, and M. Büttiker, Phys. Rev. B **54**, 8130 (1996).
[12] M. Buttiker, H. Thomas, and A. Pretre, Z. Phys. B: Condens. Matter **94**, 133 (1994).
[13] M. Buttiker, H. Thomas, and A. Pretre, Phys. Lett. A **180**, 364 (1993).
[14] M. Büttiker, J. Phys.: Condens. Matter **5**, 9361 (1993).
[15] M. Büttiker, J. Math. Phys. **37**, 4793 (1996).
[16] R. Landauer, Phys. Scr., T **42**, 110 (1996).
[17] Y. M. Blanter and M. Büttiker, Phys. Rep. **336**, 1 (2000).
[18] M. G. Vavilov, V. Ambegaokar, and I. L. Aleiner, Phys. Rev. B **63**, 195313 (2001).
[19] W. Chen, T. P. Smith III, M. Buttiker, and M. Shayegan, Phys. Rev. Lett. **73**, 146 (1994).
[20] L. H. Reydellet, P. Roche, D. C. Glattli, B. Etienne, and Y. Jin, Phys. Rev. Lett. **90**, 176803 (2003).
[21] E. A. Shaner and S. A. Lyon, Phys. Rev. Lett. **93**, 037402 (2004).
[22] J. A. Stratton, *Electromagnetic Theory* (McGraw-Hill, New York, 1941).

[23] S. Ramo, Proc. IRE **27**, 548 (1939).
[24] W. Shockley, J. Appl. Phys. **9**, 635 (1938).
[25] B. Pellegrini, Phys. Rev. B **34**, 5921 (1986).
[26] B. Pellegrini, Nuovo Cimento Soc. Ital. Fis., D **15**, 855 (1993).
[27] V. Sverdlov, X. Oriols, and K. Likharev, IEEE Trans. Nanotechnol. **2**, 59 (2003).
[28] Jörg Lehmann, S. Camalet, S. Kohler, and P. Hänggi, Chem. Phys. Lett. **368**, 282 (2003).
[29] S. Heinze, J. Tersoff, R. Martel, V. Derycke, J. Appenzeller, and Ph. Avouris, Phys. Rev. Lett. **89**, 106801 (2002).
[30] S. Camalet, J. Lehmann, S. Kohler, and P. Hänggi, Phys. Rev. Lett. **90**, 210602 (2003).
[31] P. W. Brouwer, Phys. Rev. B **58**, R10135 (1998).
[32] S. Datta and M. P. Anantram, Phys. Rev. B **45**, R13761 (1992).
[33] S. W. Kim, Phys. Rev. B **68**, 033309 (2003).
[34] M. Wagner, Phys. Rev. Lett. **85**, 174 (2000).
[35] K. C. Kulander, Phys. Rev. A **35**, R445 (1987).
[36] M. Switkes, C. M. Marcus, K. Campman, and A. C. Gossard, Science **283**, 1905 (1999).
[37] B. Altshuler and L. I. Glazman, Science **283**, 1864 (1999).
[38] The study of the electron transport in nanometric systems at few terahertz frequencies can be established without referring to a microwave or electromagnetic analysis An example where the electromagnetic propagation is included to study electron dynamics can be found in J. S. Ayubi-Moak, S. M. Goodnick, S. J. Aboud, M. Saranti, and S. El-Ghazaly, J. Comput. Electron. **2**, 183 (2003).
[39] The analytical solution for the Laplace equation with the boundary conditions $\Phi_1(\vec{r})=1$, $\vec{r}\in S_1$, and $\Phi_1(\vec{r})=0$, $\vec{r}\in S_{h\neq 1}$, defined in the volume of Fig. 2, is equal to

$$\Phi_1(x,y,z)=\frac{16}{\pi^2}\sum_{i=1,3,5,\ldots}^{\infty}\sum_{j=1,3,5,\ldots}^{\infty}\frac{\sinh[\pi\sqrt{(i/L_y)^2+(j/L_z)^2}x]}{ij\sinh[\pi\sqrt{(i/L_y)^2+(j/L_z)^2}L_x]}\times\sin\left(\frac{i\pi}{L_y}y\right)\sin\left(\frac{j\pi}{L_z}z\right)$$

All parameters are defined according to Fig. 2. Under the condition $L_x\ll L_y,L_z$ the function $\vec{F}_1(\vec{r})=-\vec{\nabla}\Phi_1(\vec{r})$ can be approximated by a constant field $\vec{F}_1(\vec{r})=-(1/L_x)\vec{x}$ with $|\vec{x}|=1$. Obviously, this approximation is not accurate for positions close to the surfaces that are parallel to the transport direction, but such deviations are not meaningful as long as $L_x\ll L_y,L_z$. [N. Ida, *Engineering Electromagnetics* (Springer-Verlag, New York, 2000)].
[40] L. Varani, L. Reggiani, T. Kuhn, T. Gonzalez, and D. Pardo, IEEE Trans. Electron Devices **41**, 1916 (1994).
[41] D. Bohm, Phys. Rev. **85**, 166 (1952).
[42] P. R. Holland, *The Quantum Theory of Motion* (Cambridge University Press, Cambridge, U.K., 1993).
[43] X. Oriols, F. Martín, and J. Suñé, Phys. Rev. A **54**, 2594 (1996).
[44] J. Suñé and X. Oriols, Phys. Rev. Lett. **85**, 894 (2000).
[45] The sum over the velocities of N particles, at time t, in the classical expression of the Ramo-Shockley theorem, $I(t)=(q/L)\Sigma_{i=1}^{N(t)}v_i(x,t)$, can be related to a double integral over all initial times and over all positions inside the device, $\Sigma_{i=1}^{N(t)}\rightarrow C\int_{-\infty}^{t}dt_j\int_0^L dx|\Psi_{t_j}(x,t)|^2$. By using the Bohm definition of the electron velocity, $v_{tj}(x,t)=J_{t_j}(x,t)/|\Psi_{t_j}(x,t)|^2$, we obtain expression (10) which is the main result of this work.
[46] In principle, it would be possible to generalize our model to a many-particle system within the first-quantization framework by simply dealing with an antisymmetrical many-particle wave function. Let us mention that we explicitly consider the Pauli principle in the contact region (through the injection rate), but we neglect its effect inside the device active region. Hard computational requirements are the only limitation to the solution of the many-particle wave function. The computation of the N-particle wave function through a finite-difference scheme of the Schrödinger equation for a system length of 100 nm (a spatial step of 0.1 nm) involves solving roughly 10^{3N} unknowns.
[47] In general, the Floquet approach is applied to compute the dc response to an ac driving potential, where it is assumed that the displacement current vanishes in average.
[48] A quite preliminary step in this direction can be found in X. Oriols, A. Trois, and G. Blouin, Appl. Phys. Lett. **85**, 3596 (2004), where the Poisson equation and the Schrödinger equation are solved self-consistently.
[49] Since the Schrödinger equation (A1) determines the temporal variations of the wave function, the time derivative of the probability presence $\rho'=\Psi(\vec{r},t)\Psi^*(\vec{r},t)$ is equal to $i\hbar\partial\rho'/\partial t=-\hbar^2/2m[\Psi^*(\vec{r},t)\nabla^2\Psi(\vec{r},t)-\Psi(\vec{r},t)\nabla^2\Psi^*(\vec{r},t)]$. By defining the particle current density from Eq. (B15) we obtain $\partial\rho'/\partial t+\vec{\nabla}\cdot\vec{J}_c'=0$ (See Ref. 53).
[50] The divergence of the Maxwell generalization of the Ampèere law, $\vec{\nabla}\times\hat{H}=\vec{J}_c+\partial\vec{D}/\partial t$, is equal to zero because the divergence of a rotational is null. Therefore, $\vec{\nabla}\cdot(\vec{J}_c+\partial\vec{D}/\partial t)=0$ and from the Gauss law $\vec{\nabla}\vec{D}=\rho$, we obtain $\partial\rho/\partial t+\vec{\nabla}\cdot\vec{J}_c=0$ (see Ref. 22).
[51] The evolution of the average energy is determined by the expression $(d/dt)\langle\hat{H}\rangle=\langle\partial\hat{H}/\partial t\rangle$ where the average value is defined as $\langle\hat{A}\rangle=\int\Psi^*(\vec{r},t)\hat{A}(\vec{r},t)\Psi(\vec{r},t)d\vec{r}$ for a wave function $\Psi(\vec{r},t)$ and an operator $\hat{A}(\vec{r},t)$ in the coordinate representation.
[52] A. M. Kriman, N. C. Kluksdahl, and D. K. Ferry, Phys. Rev. B **36**, 5953 (1987).
[53] C. Cohen-Tanoudji, B. Diu, and F. Laloë, *Quantum Mechanics* (Wiley, New York, 1977).
[54] L. S. Levitov, H. Lee, and G. B. Lesovik, J. Math. Phys. **37**, 4845 (1996); L. S. Levitov and G. B. Lesovik, JETP Lett. **58**, 230 (1993).
[55] X. Oriols, F. Martín, and J. Suñé, Appl. Phys. Lett. **79**, 1703 (2001); **80**, 4048 (2002); X. Oriols, IEEE Trans. Electron Devices **50**, 1830 (2003).
[56] As an evident example, we consider the time-dependent potential $U(x,t)=K(x)\delta(t-t_0)$ where $K(x)$ is a square function defined as $K(x)=1$ eV at $0<x<L$ and zero elsewhere. Then, wave packets with central velocity v_0 defined at $t=0$ at a central initial position $x_0\approx-v_0t_0$ will be reflected by the barrier $U(x,t_0)=1$ eV and we will obtain $T^S(E)\approx 0$. On the contrary, identical wave packets with the same central velocity v_0 but different initial central position ($x_0\gg-v_0t$ or $x_0\ll-v_0t$) will traverse the active device region without "seeing" the square barrier; thus $T^S(E)\approx 1$.
[57] For wave packets with a large spatial dispersion $\sigma_x=a/\sqrt{2}$, like the ones considered in this work, we can assume that $a^2\gg 2\hbar(t-t_j)/m$ in expression (A5). Then, the initial wave packet with initial position (x_0+d) and initial time t_j is identical to the initial wave packet with initial position x_0 and initial time $(t_j+\hbar k_c d/m)$. The only difference between the two wave packets is a useless global phase $\exp(ik_c d)$.
[58] We assume that under time-dependent potential profiles the final-state blocking factor $[1-f^{D/S}(E)]$ is not needed in expression

(13). This is an accurate assumption at least for linear ac conductance (see Refs. 11–15).

[59] R. Landauer, IBM J. Res. Dev. **1**, 223 (1957).

[60] S. Datta, *Electronic Transport in Mesoscopic Systems* (Cambridge University Press, Cambridge, U.K. 1995).

[61] A. Bruce-Carlson, *Communication Systems* (McGarw-Hill International Editions, New York, 1986).

[62] The wave packet spatial dispersion is equal to $\sigma_x = a/\sqrt{2} = 30$ nm [see Eq. (A5)], much larger than the device length $L = 15$ nm. Thus, the wave packet width in the wave vector space is $\sigma_k = 1/\sigma_x = 33 \times 10^6$ m^{-1}. Then, for a wave packet with central energy around $E = 0.1$ eV (central vector $k = \sqrt{2mE/\hbar} = 0.72 \times 10^9$ m^{-1}) we obtain $\sigma_E = (\hbar^2 k/m)\sigma_k \approx 0.01$ eV for the Si light electron effective mass. Hence, our injected wave packets will be quite similar to those monoenergetic wave functions used in the other formalisms.

[63] In principle, there is no restriction for the energy uncertainty associated with an electron moving in a semiconductor. For example, monoenergetic wave functions (without energy uncertainty) are used to describe electrons in the well-known Landauer model (Ref. 59), even if this selection results in unbounded states at infinity. The Floquet formalism also defines injection electrons as monoenergetic states (Refs. 1–4).

[64] In the practical computation, the range of initial times that we have to compute is not $-\infty < t_j < t$, but a more restricted range. We only consider j wave packets whose probability presence is not negligible in the system at time t. Those j wave packets that have not arrived yet, or have already left the system, at the time t are not explicitly simulated.

[65] S. Brouard and J. G. Muga, Phys. Rev. Lett. **81**, 2621 (1998).

[66] R. Landauer and Th. Martin, Rev. Mod. Phys. **66**, 217 (1994).

[67] X. Oriols, F. Martín, and J. Suñé, Solid State Commun. **99**, 123 (1996).